# Optimal spacing and penetration of cracks in a shrinking slab

D. R. Jenkins*
*CSIRO Mathematical and Information Sciences, Locked Bag 17, North Ryde, NSW 1670, Australia*
(Received 13 October 2004; published 23 May 2005)

A method based on energy minimization is used to determine the spacing and penetration of a regular array of cracks in a slab that is shrinking due to a changing temperature field. The results show a range of different crack propagation behavior dependent on a single dimensionless parameter, being the ratio of the slab thickness and a characteristic length for the material. At low parameter values the minimum energy state can be achieved by continually adding more cracks until a steady state is achieved. At higher values, a minimum crack spacing is reached at finite time, beyond which the cracks are constrained to propagate with the minimum spacing. In the latter case, the uniform propagation is potentially unstable to a spatial period doubling, leading to increasingly complex crack penetration patterns. The energy minimization combined with the period doubling instability provides a means of determining the minimum energy state of cracks for all time. The problem considered here can be seen as a paradigm for cracking phenomena that occur on a large range of scales, from planetary to microscopic.

DOI: 10.1103/PhysRevE.71.056117 PACS number(s): 62.20.Mk, 46.50.+a

## I. INTRODUCTION

There is a range of phenomena associated with the shrinkage of materials which lead to arrays of more-or-less regularly spaced cracks. Common examples of regular crack arrays in thin layers of material are paints, glazing and other coatings that have been deposited on substrates [1–3], while deeper crack arrays are observed in situations such as road paving [4,5], concrete [6], drying of mud [7,8], soil [9] food [10] and timber [11] or the formation of basalt columns [12,13] and other geological features both terrestrial and extra-terrestrial [14,15]. There is often remarkable uniformity in both the spacing and penetration of cracks. In some cases the existence of cracks may be desirable, such as in soil, since they assist the infiltration of water, or undesirable, such as in many of the thin coating applications referred to above. Thus it may be useful to know, first, whether a layer of material that is undergoing shrinkage will crack at all, or whether its mechanical properties are such that it can accommodate the stress associated with the shrinkage. Secondly, should such a material crack in a regular array, it may be valuable to know the separation between the cracks and the extent of their penetration.

A particular example where the spacing between cracks has economic significance is the process of formation of coke from crushed coal. Coke is used in the iron-making blast furnace as part of the conventional steelmaking process. It is a lump material that is formed by the fusion of crushed coal particles in a coke oven. The coke shrinks and a regular array of cracks propagates in the direction of the temperature gradient in the coke oven. The coke breaks into lumps whose mean size depends on the mean spacing of the cracks. Both the mean and distribution of lump sizes is important in the performance of coke in the blast furnace, so the ability to predict or control the crack spacing is of some importance [16].

There are several studies of the propagation of crack arrays under various conditions. Nemat-Nasser *et al.* [17,18], Bažant *et al.* [19], and Bahr *et al.* [20,21] considered the propagation of a regular array of cracks with a specified spacing, including their stability. They showed that a regular array of cracks having uniform penetration into a sample will propagate uniformly until a critical state is reached, at which every second crack stops growing. Using slightly different approaches, each of the above determined and evaluated the stability criterion for this critical state, which is based on the change of sign of the second derivative of the strain energy with respect to the crack penetration. In each of these studies the spacing between the cracks was assumed, rather than being determined from the model system.

This paper presents a method, based on energy minimization of an array of cracks, for determining the optimal spacing and penetration of the cracks as they form under the effects of shrinkage. The aim is to determine the most likely configuration of cracks and their progression with time.

## II. MODEL FORMULATION AND SOLUTION

Consider the situation depicted in Fig. 1, where a slab having constant material and thermal properties and initially at uniform temperature $T_0$, is subject to a sudden change of temperature $\Delta T$ at the surface $z=1$. Then, assuming heat transfer by conduction alone, the temperature at any time $t$ after the sudden temperature change is given by [22]

$$T(x,t) = T_0 + \Delta T z + 2\Delta T \sum_{n=1}^{\infty} \frac{\cos n\pi \sin n\pi z}{n\pi} e^{-n^2\pi^2 t}, \quad (1)$$

where the distance $z$ has been scaled with the slab thickness, $L$, the time $t$ has been scaled with the thermal diffusion time

$$\tau = \frac{L^2}{\kappa}$$

and $\kappa$ is the thermal diffusivity of the slab.

*Electronic address: David.R.Jenkins@csiro.au

 

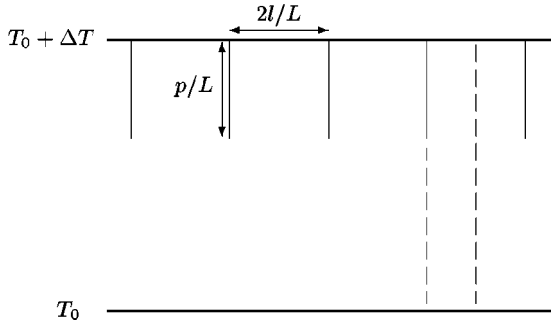


FIG. 1. Geometry of a slab with an array of regularly spaced cracks, propagating from the top bounding surface. Dashed lines denote the representative geometry used in the finite element calculations.

Assuming that the material behaves thermoelastically, the equations of mechanical equilibrium are

$$\frac{\partial \sigma_{ij}}{\partial x_i} = 0, \tag{2}$$

where

$$\sigma_{ij} = \lambda(e - 3\alpha(T - T_0))\,\delta_{ij} + 2\mu(\epsilon_{ij} - \alpha(T - T_0)\,\delta_{ij}) \tag{3}$$

are the components of stress, $\lambda$ and $\mu$ are the Lamé coefficients,

$$\mu = \frac{Y}{2(1+\nu)}, \quad \lambda = \frac{2\mu\nu}{1-2\nu},$$

$Y$ is Young's modulus, $\nu$ is the Poisson ratio, $\alpha$ is the coefficient of thermal expansion,

$$\epsilon_{ij} = \frac{1}{2}\left(\frac{\partial u_i}{\partial x_j} + \frac{\partial u_j}{\partial x_i}\right)$$

are the strain components, $u_i$ are displacements and

$$e = \epsilon_{ii}.$$

The model equations assume quasistatic equilibrium, implicit in which is that the crack propagation occurs at a faster rate than the diffusion process. A corollary is that the dynamics of crack propagation are not as significant as their energetics. Also, the model assumes that the time for nucleation of cracks is smaller than the diffusion time scale.

From these equations it can be shown that the local strain energy density $U$ is given by

$$U = \frac{1}{2}\lambda e^2 + \mu\epsilon_{ij}\epsilon_{ij} - (2\mu + 3\lambda)\alpha(T - T_0)e + \left[\frac{9\lambda}{2} + 3\mu\right][\alpha(T - T_0)]^2 \tag{4}$$

and the total strain energy of the slab is given by

$$S = \int_V U dV. \tag{5}$$

In the case when the slab contains a regular array of mode I (opening) cracks of spacing $2l$ and penetration $p$, the total energy of the slab per unit length is

$$E = \frac{S}{l} + \eta\frac{p}{l}, \tag{6}$$

where the second term is due to the energy required to open up the cracks, which is assumed to be proportional to $p$. By appropriate nondimensionalization, Eq. (6) becomes

$$E'(l,p) = \frac{E}{\eta} = \left[\frac{(\alpha\Delta T)^2 YL}{\eta}\right]\frac{S'}{l} + \frac{p}{l}. \tag{7}$$

The basic approach here is that the spacing and penetration of the cracks in the regular array are such that, at any given time, they minimize $E'$ [17,18,23]. The minimization is achieved by first determining the dependence of $E'$ on $l$ and $p$, which requires solving Eqs. (2) with appropriate boundary conditions and determining $S'(l,p)$ from Eq. (5).

Note that $E'$ depends upon the single dimensionless quantity,

$$\frac{L}{L_c} = \frac{(\alpha\Delta T)^2 YL}{\eta},$$

where $L_c$ is a characteristic length of the material,

$$L_c = \frac{\eta/Y}{(\alpha\Delta T)^2},$$

which depends on its relative brittleness, $\eta/Y$, and (the square of) its total shrinkage $\alpha\Delta T$ for a given temperature difference. $L_c$ is the Griffith crack length for a shrinking solid, and its significance is that cracking will occur when diffusion of heat has penetrated the slab to a depth of roughly $L_c$ [24].

Assuming that the temperature field is not affected by the location of cracks, then the one-dimensional equation (1) is valid for all time. This is substituted into Eqs. (2), which are solved for each time, in order to evaluate the strain energy integral, Eq. (5).

Note that temperature is used here as the driver of the shrinkage, but it could equally well be any other diffusive phenomenon, such as drying or volatile transport.

### Numerical solution

Since the slab thickness is finite, it is convenient to use the finite element method for solution of equations (2) and appropriate boundary conditions. A representative portion of the geometry, taking into account the symmetry, is denoted by the dashed lines in Fig. 1 and this is used for the calculations. Figure 2 shows the specific boundary conditions used in the calculations. They are that the slab is fixed at the bottom surface, but free at the top and along the crack surface. There are symmetry conditions along the remainder of the boundary. The particular conditions used relate to, for example, a shrinking slab of material that is fixed to a very stiff substrate maintained at constant temperature, and being cooled at its free surface.

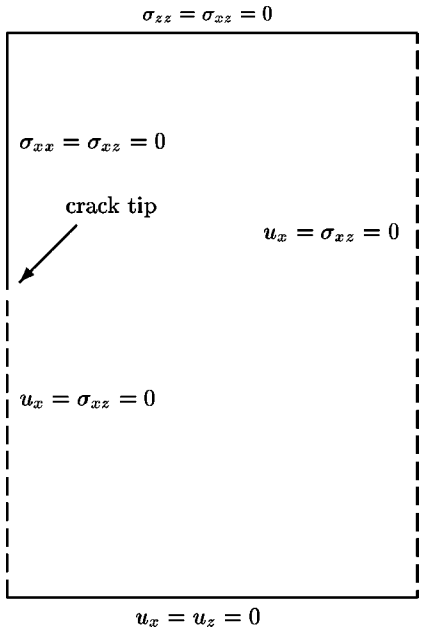


FIG. 2. Boundary condition specification. The solid lines are actual surfaces of the slab and the dashed lines are symmetry planes.

The general purpose finite element package *Fastflo* is used for the numerical solution. The in-built unstructured mesh generator has the ability to concentrate the mesh at specific points. The mesh concentration is used to accurately resolve the stress singularity at the crack tip.

The methodology used to determine $E'(l,p)$ is, for a given time $t$, to solve the displacement equations and evaluate $S'(l,p)$ for a range of values of $l$ and $p$ as

$$S'_{mn} = S'(l_m, p_n), \quad m = 1 \ldots M, \quad n = 0 \ldots N, \tag{8}$$

where

$$l_m = m\frac{\Delta l}{L}, \quad p_n = n\frac{\Delta p}{L}$$

and

$$\frac{\Delta l}{L} = \frac{2}{M} \text{ and } \frac{\Delta p}{L} = \frac{1}{N}.$$

Typically $M = N = 40$ was used, meaning that 1640 evaluation of $S'$ were obtained. For each evaluation, the number of finite element nodes was proportional to the area of the geometry, so that approximately equivalent accuracy was maintained over all the evaluations of $S'$. Notice that the maximum value of $l/L$ used is 2 (i.e., 4 times the slab thickness), which from experience is sufficient to obtain the minimum energy state. The calculations allow a regular grid of values of $E'$ over $l$ and $p$ to be determined for any value of $L/L_c$, and biquadratic interpolation was used to determine the global minimum of $E'(l,p)$, which occurs at $(l_0, p_0)$. All the results shown here are for $\nu = 0.3$.

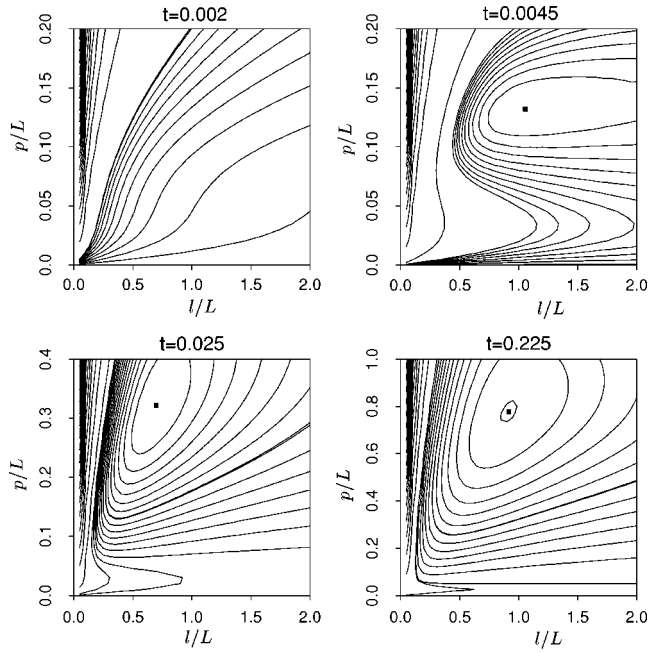


FIG. 3. Contour plots of $E'(l,p)$ for various times (marked on each graph) when $L/L_c = 6$. The square dot in 3 of the graphs indicates the location $l_0/L, p_0/L$ which minimizes $E'$. Note that the contour spacing is small near the minimum compared to the remainder of the graph.

## III. RESULTS AND DISCUSSION

### A. Spacing and penetration

Figure 3 shows contour maps of $E'(l,p)$ at various times, for $L/L_c = 6$. At $t = 0.002$, the minimum $E'$ occurs when $p = 0$, i.e. without any cracks at all, so that the material is able to shrink without cracking. However, at $t = 0.0045$ the minimum shifts to an array of cracks with finite penetration and at later times the minimum point moves in the direction of increased penetration. An alternative display of $(l_0, p_0)$ is shown in Fig. 4, where their variation with time is plotted explicitly.

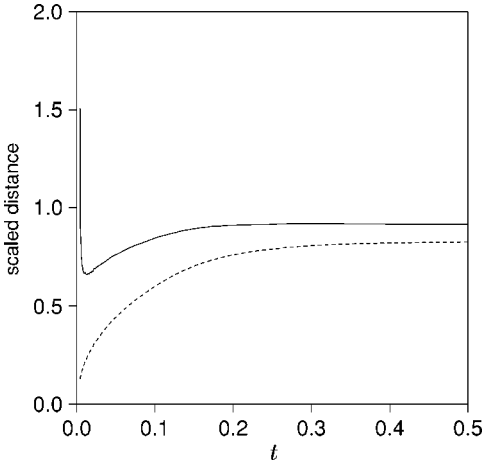


FIG. 4. Graphs of $l_0/L$ (solid line) and $p_0/L$ (dashed line), versus $t$ for $L/L_c = 6$.

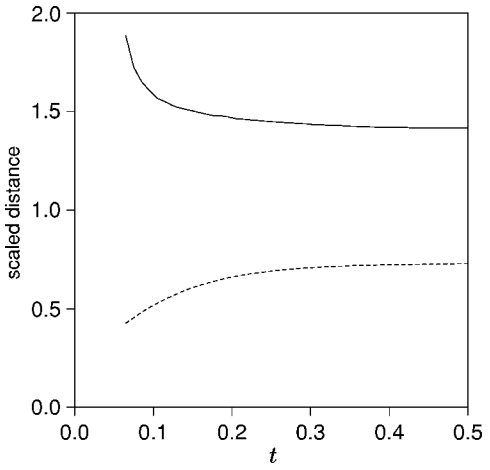


FIG. 5. Graphs of $l_0/L$ (solid line) and $p_0/L$ (dashed line), versus $t$ for $L/L_c=2$.

This graph shows that, until $t\approx 0.004$ the material does not crack, but thereafter it will crack. Immediately after this time, the minimum energy configuration is for large crack spacing, but this reduces with time until $t\approx 0.013$, when $l_0/L\approx 0.66$ and $p_0/L\approx 0.23$. For later times the minimum energy state is a spacing which is greater than that at $t=0.013$, but with ever increasing penetration. So the minimum crack spacing is about 1.33 times the slab thickness, with the cracks penetrating almost $1/4$ of the slab thickness. For large time, the spacing and penetration approach an asymptote with $l_0/L\approx 0.92$ and $p_0/L\approx 0.83$, so the cracks never penetrate all the way through the slab.

Figure 5 shows the graph of $(l_0/L, p_0/L)$ versus time for $L/L_c=2$. In this case no cracks will appear until around $t=0.06$ but when they do appear, they penetrate almost halfway through the slab. Thereafter, the minimum energy spacing continues to decrease, without having a minimum value as in the $L/L_c=6$ case.

Figure 6 shows the graph of $(l_0/L, p_0/L)$ versus time for $L/L_c=16$. In this case cracking occurs very early, around $t=0.0006$ and the minimum energy spacing decreases to

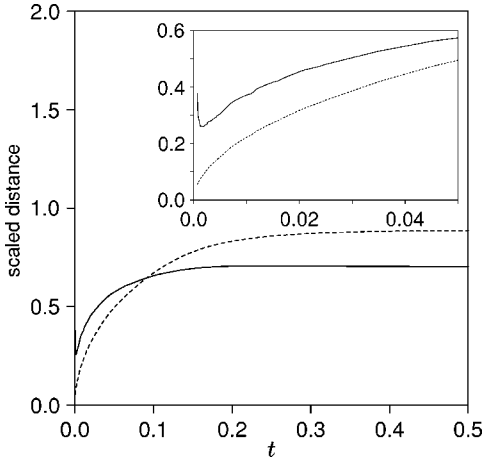


FIG. 6. Graphs of $l_0/L$ (solid line) and $p_0/L$ (dashed line), versus $t$ for $L/L_c=16$. The inset shows an expanded view of the behavior at small time.

$l_0/L\approx 0.27$ at which stage $p_0/L\approx 0.1$ at $t=0.0022$. In other words, the minimum crack spacing is about half the slab thickness, but the penetration of the cracks is small. For later times, $l_0$ increases significantly to plateau at a value considerably more than twice the minimum crack spacing.

The results show two different regimes of crack behavior, depending on $L/L_c$. For low $L/L_c$ no cracks appear for a relatively long time, but when they do appear they penetrate a long way through the slab. Because $l_0$ decreases monotonically with time, additional cracks are likely to appear in order to achieve a situation as close as possible to the minimum energy configuration. This process should continue until a steady state is reached. This then completely describes the crack propagation behavior for low $L/L_c$.

For $L/L_c$ above about 2.5, the curves of $l_0$ against $t$ have a minimum value, which is denoted $l_{0m}$ occurring at $t_m$. At that time, there is a corresponding $p_{0m}$. For $t>t_m$, the minimum energy configuration can only be achieved by some mechanism of crack coarsening, since the slab will already contain cracks that are more closely spaced than the minimum energy configuration. In order to achieve this, some cracks must either stop, recede or even disappear completely while others continue to propagate. While the latter two possibilities cannot be completely ruled out, it has been shown by several authors, including Nemat-Nasser *et al.* [17], that a regular crack array, once formed, will propagate stably, with each of the cracks maintaining the same length, provided that

$$\frac{\partial^2 S'(l,p)}{\partial p^2} > 0 \tag{9}$$

for a fixed value of $l$, and that it will lose stability to a state where every second crack stops propagating while every other one continues, when $\partial^2 S'/\partial p^2$ changes sign. As a result, the most likely scenario is that cracks with minimum spacing, $l_{0m}$, achieved at $t_m$, will continue to propagate for $t>t_m$ in order to relieve the stress built up as the material continues to shrink, subject to the above instability. Thus the minimum in the $l_0$ vs $t$ curve defines a unique optimal value of the crack spacing, which is $2l_{0m}$. It is this crack spacing that would ultimately be observed on the surface of the slab, regardless of the further propagation history of the cracks.

The remainder of the paper is concerned with the propagation and stability of cracks for $t>t_m$ in cases where $t_m$ exists, i.e., for $L/L_c$ larger than about 2.5.

### B. Propagation of optimally spaced cracks

For values of $L/L_c>2.5$ the energy minimization approach can be used to determine the propagation of optimally spaced cracks, starting from $(l_{0m}, p_{0m})$ at $t=t_m$. In such cases, $E'(l_{0m}, p)$ is minimized with respect to $p$ to find the optimal (minimum energy) penetration, $p_m$ for cracks of spacing $2l_{0m}$ for $t>t_m$. Figure 7 shows a graph of the calculated $p_m$ versus $t$ for $L/L_c=16$ with a continual increase in penetration as $t$ increases. The energy for the state $[l_{0m}, p_m(t)]$ is clearly higher than that for the state $[l_0(t), p_0(t)]$ for $t>t_m$ in this case, so is potentially unstable, as described earlier. A numerical estimate of $\partial^2 S'/\partial p^2$ is obtained from the difference

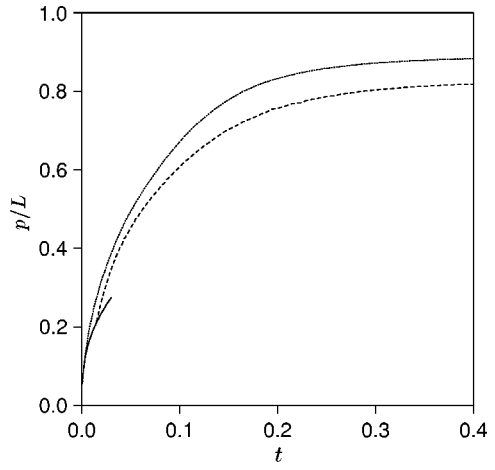


FIG. 7. Graph of $p_m$ vs $t$ for cracks with spacing $2l_{0m}$, when $L/L_c=16$. The solid line is for the case when all cracks propagate together, while the dashed line is when every second crack has stopped, after $t_{m1}$. The dotted line is a graph of $p_0$ versus $t$.

$$\frac{S'(l_{0m},p_m(t)) - S'(l_{0m},p_m(t);\delta)}{\delta^2}, \tag{10}$$

where $S'(l_{0m},p_m(t);\delta)$ is the strain energy of a state in which the penetration of every second crack is $p_m+\delta$ and of every other crack is $p_m-\delta$ [23]. Figure 8 shows a graph of this difference for $t>t_m$ when $L/L_c=16$, calculated using $\delta=0.1p_m(t)$. It is difficult to obtain an accurate numerical value of $\partial^2 S'/\partial p^2$ due to the stress singularity at the crack tip. A value of $\delta$ proportional to $p_m(t)$ was used as it was found that too small a value leads to poor resolution of the effect of the two stress singularities, while too large a value leads to a poor approximation to the second derivative. The results show that $\partial^2 S'/\partial p^2$ changes sign at $t=t_{m1}\approx 0.0144$, indicating that the regular array of cracks with spacing $l_{0m}$ loses stability in the form of the spatial "period doubling" described above. For $t>t_{m1}$, every second crack continues to propagate and the penetration satisfying the energy minimization criterion for this case is also shown in Fig. 7. This was calculated by minimising $E'$ with respect to $p$, taking into account that every second crack stopped propagating at $t_{m1}$. The propagation occurs at a higher rate, at least initially, for the new configuration.

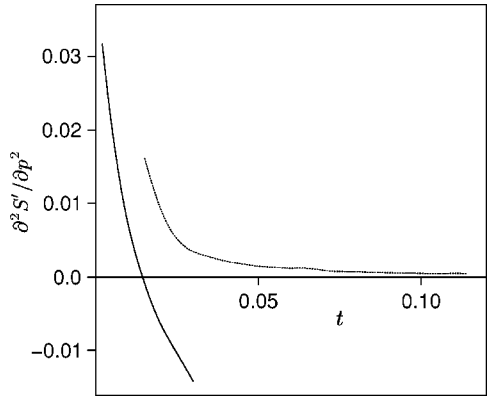


FIG. 8. Graph of $\partial^2 S'/\partial p^2$ vs $t$ for $L/L_c=16$. The solid line is for equal length cracks and the dotted line for every second crack stopped, $t>t_{m1}$.

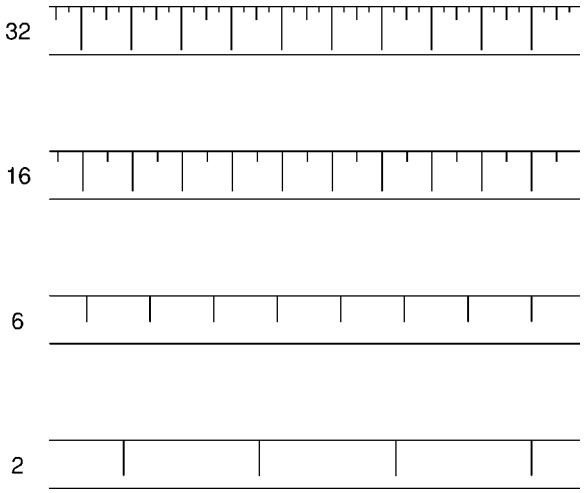


FIG. 9. Schematics of the final crack states for different $L/L_c$, whose value is shown next to each configuration.

The process can be repeated, with the array of $4l_{0m}$ spaced propagating cracks having every other crack stationary with penetration $p_m(t_{m1})$ potentially becoming unstable to a situation where every fourth crack stops and only those separated by $8l_{0m}$ continue to propagate. However, the calculated second derivative of the strain energy for this state does not change sign, indicating that there will not be another period doubling for this case. This is not surprising, since Fig. 6 shows that the asymptotic value of $l_0$ is less than $4l_{0m}$.

The same procedure was followed for $L/L_c=32$, in which case a period doubling occurs at $t_{m1}\approx 0.0035$ and a second at $t_{m2}\approx 0.0195$. Accurate resolution of the strain energy and the stability criterion becomes more difficult as $L/L_c$ increases using the present approach, but it seems most likely that further doublings are possible at higher values. The results show that the effect of the period doubling cascade is to bring the already cracked material closer to the minimum energy state associated with uniformly penetrating cracks.

After having carried out the energy minimisation and evaluated the stability criterion as time progresses, it is possible to determine the crack configuration at large time, when the temperature field has reached a steady state and the cracks are no longer propagating. Figure 9 shows schematics of the final crack configurations for 4 different values of $L/L_c$. Each configuration is achieved by a different cracking route.

For $L/L_c=2$, the set of uniformly spaced cracks with uniform penetration is achieved by addition of extra cracks as time proceeded.

For $L/L_c=6$ a similar state is achieved via a similar route until a minimum spacing is reached, after which cracks at the minimum spacing propagate together. Note that the crack spacing is smaller in this case, as is the final crack penetration, compared to $L/L_c=2$.

For $L/L_c=16$, the state of equally spaced cracks having alternating penetration is achieved by a similar route to the $L/L_c=6$ case until the uniform spaced cracks become un-

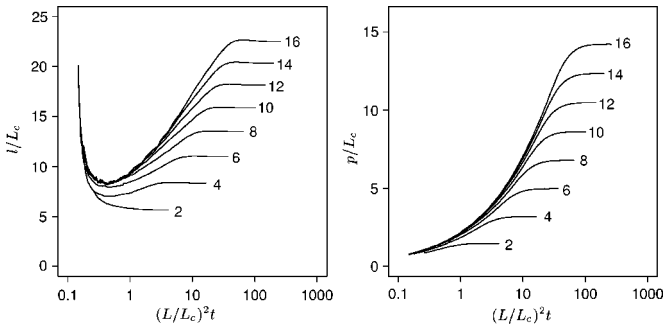


FIG. 10. Graphs of $l/L_c$ and $p/L_c$ vs $(L/L_c)^2t$ for varying $L/L_c$. The values of $L/L_c$ are shown beside each curve. A logarithmic scale has been used to clearly illustrate the small time behavior.

stable, after which every second crack propagates.

For $L/L_c=32$, the state of equally spaced cracks having 3 different penetration depths is achieved by a second instability, so that ultimately only every fourth crack propagates.

The schematics in Fig. 9 could be interpreted as a set of layers of different material, with the brittleness of the material increasing with $L/L_c$. In that case it seems that as the brittleness increases there is a set of "principal" cracks whose spacing does not change with brittleness, but the other, less penetrating cracks become closer together. The $L/L_c=32$ example gives the impression of crazing on the surface of a brittle material with occasional deep cracks, while the $L/L_c=2$ example gives the impression of cracking of a more ductile material. Alternatively, they could be interpreted as a set of layers of the same material, but with increasing amounts of shrinkage with $L/L_c$. As the shrinkage increases, the crack spacing observed on the surface reduces and the complexity of the pattern of penetration increases.

### C. Effect of slab thickness

The scalings used above are covenient for computation, but it is useful to rescale the results to consider the effect of different slab thickness on the crack spacing and penetration. The scaled crack spacing, $l/L$, and penetration, $p/L$, when multiplied by $L/L_c$ are dependent only on the material properties and similarly for the scaled time, $t$, when multiplied by $(L/L_c)^2$. Figure 10 shows graphs of $l/L_c$ and $p/L_c$ against $(L/L_c)^2t$, for different values of $L/L_c$, showing the effect of varying the slab thickness for a given material. For a thin slab, there is no minimum in the $l/L_c$ curve, but for thicker slabs the minimum appears.

Notice that the minimum crack spacing approaches a limiting value as $L/L_c$ increases, as does the time at which the minimum crack spacing occurs. Thus the crack spacing observed on the surface of a slab becomes independent of the slab thickness, but the spacing further into the slab may be different, due to the effect of the period doubling phenomenon, as shown by the schematics in Fig. 11. The results indicate that there is a minimum crack spacing for cracks propagating into a semi-infinite slab, represented by the limit $L/L_c\to\infty$. In such a case, there will be surface cracks at the minimum spacing, but further into the sample the crack spacing will continue to increase via the period doublings. Eventually, the spacing will be sufficiently large that the cracks will be essentially independent.

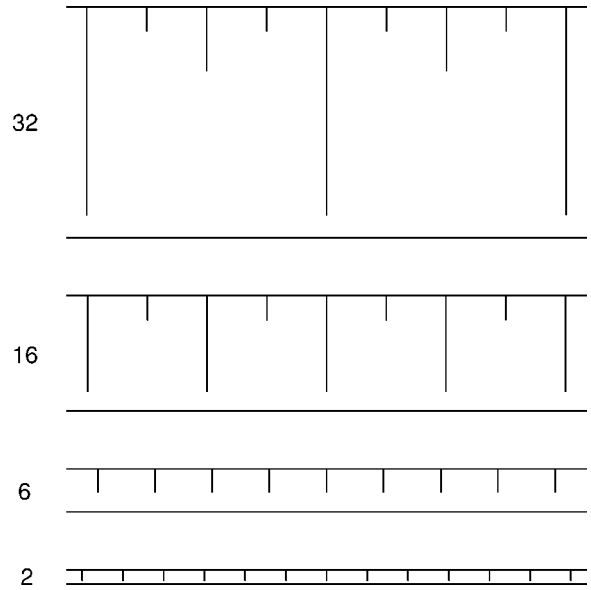


FIG. 11. Schematics of the final crack states for different $L/L_c$, representing different slab thickness, whose value is shown next to each configuration.

Also, notice that the cracks appear at about the same time, with the same penetration, for sufficiently large $L/L_c$, which is to be expected since this is the scaled time at which the length scale associated with diffusion of heat is comparable with the Griffith crack length, $L_c$. At this time, there is sufficient stress due to shrinkage to overcome the energy barrier between the uncracked and cracked state. This barrier is evident in the contour plots of Fig. 3.

The experiments of both Groisman and Kaplan [25] and Shorlin *et al.* [26] show increasing crack spacing with depth. Although it is not stated by the authors, the results of Shorlin *et al.* (their Fig. 9) may indicate that the crack spacing is approaching a limiting value.

### D. Limiting behavior

At steady state the numerical results show that the crack spacing $l/L_c\sim(L/L_c)^{3/4}$ and $p/L_c\sim L/L_c$ as $(L/L_c)\to\infty$. The latter can be understood because the cracks follow the heat diffusion and the former can be derived from a simple scaling analysis, along the lines of that given by Brener *et al.* [27]. For $(L/L_c)\gg 1$ (at values larger than shown in the graphs here), the crack penetration greatly exceeds the crack spacing. In that case, the regions between each crack can be considered as thin plates, with the exception of the region near the crack tip. Then the bending of those plates is described by the fourth order equation

$$\frac{8Yl^3}{12(1-\nu^2)}\triangle^2 u_x = Y\alpha\Delta T, \tag{11}$$

where $\triangle$ is the two-dimensional Laplacian. The term on the right-hand side is a measure of the stress in the plates due to the shrinkage. This then leads to an order relation for $u_x$ of

$$u_x \sim \frac{\alpha \Delta T p^4}{l^3} \tag{12}$$

and the change in volume due to the opening of the crack is then

$$V \sim \frac{\alpha \Delta T p^5}{l^3}, \tag{13}$$

which results in a release of elastic energy per plate of

$$W_e \sim -Y\alpha\Delta T V \sim -\frac{Y(\alpha\Delta T)^2 p^5}{l^3}.$$

This, when combined with the energy asociated with crack opening and scaled by $\eta l$, gives

$$\Delta E' = A\frac{p}{l} - B\frac{p^5}{L_c l^4} \tag{14}$$

for some unknown constants $A$ and $B$. For local equilibrium, minimization of $E'$ with respect to $l$ is required, giving

$$l^3 L_c \sim p^4 \tag{15}$$

which, when $l$ and $p$ are scaled with $L_c$ gives the observed limiting behavior when taking into account that $p \sim L$.

In fact, the numerical results show that the limiting behavior holds over a large range of $L/L_c$ for the steady state solutions, only deviating at small $L/L_c$. Nevertheless, $l/L_c$ decreases monotonically down to low values of $L/L_c$, and this helps to explain why there is a minimum in the crack spacing for large $L/L_c$ but not for small $L/L_c$, since the crack spacing is always decreasing at early times, but must then rise again as $t \to \infty$ for $L/L_c$ above some particular value (about 2.5 from the numerical results) in order to achieve the limiting behavior.

## IV. CONCLUDING REMARKS

The approach taken here provides a mechanism for determining a unique value for the most likely minimum crack spacing in regular crack arrays associated with shrinkage. The two possibilities identified are as follows.

(1) For low $L/L_c$ the minimum spacing only occurs at the end of shrinkage ($t \to \infty$), with a succession of additional cracks being added until this time.

(2) For $L/L_c$ greater than some critical value (about 2.5 for the configuration discussed here), the minimum spacing occurs at a finite time, $t_m$. There after, cracks will propagate uniformly with that minimum spacing, subject to a potential spatial period doubling instability.

The combination of the minimum energy approach with the identification of a minimum crack spacing and its resultant constraint on further propagation, along with the stability criterion for uniformly propagating cracks, allows determination of the minimum energy crack configuration for all of the shrinkage time. Hence the final state of the cracked material can be determined.

No consideration has been given here to the initial crack formation, or indeed the mechanism of adding extra cracks at early times, before the minimum crack spacing is reached. Presumably, a mechanism of halving crack spacing, as a kind of symmetrical analogy to the period doubling that occurs at later time, is possible. This is mostly of interest at low $L/L_c$ where the process occurs gradually, compared to higher values where the minimum spacing occurs in a short time relative to the time required for diffusion of heat.

Although only a simple geometry has been considered here, with specific boundary conditions, it is likely that similar behaviour will occur in other configurations. Moreover, it is expected that the same behaviour will be found for the 3 dimensional situation, and this has been observed (including the spatial period doubling) in experiments on starch columns [28–30] and coke formation [31]. The computations associated with 3D, along with the topological issues of the crack pattern, are more formidable, but progress on simple geometries should be possible. While there is experimental evidence that the kind of crack patterns predicted here exist, it is difficult to make quantitative comparisons of crack spacings and penetration in a particular example. In order to do this, more realistic boundary conditions, along with good estimates of the material properties are necessary. The motivation for this work arose out of a study of coke formation, and such data is not currently readily available. Moreover, coke formation has the added complication that the coke slab is growing in thickness. Nevertheless, the aim is to develop a quantitative crack spacing predictive capability.

## ACKNOWLEDGMENTS

Useful discussions with Dr. Frank de Hoog of CSIRO are gratefully acknowledged.

[1] M. S. Hu and A. G. Evans, Acta Metall. **37**, 917 (1989).
[2] P. J. Parbrook, T. Wang, M. A. Whitehead, C. N. Harrison, R. J. Lynch, and R. T. Murray, Phys. Status Solidi C, **0**, 2055 (2003).
[3] B. D. Choules, K. Kokini, and T. A. Taylor, Mater. Sci. Eng., A **299**, 296 (2001).
[4] A. P. Hong, Y. N. Li, and Z. P. Bažant, J. Eng. Mech. **123**, 267 (1997).
[5] D. H. Timm, B. B. Guzina, and V. R. Voller, Int. J. Solids Struct., **40**, 125 (2003).
[6] Z. P. Bažant, J-K. Kim, and S-E. Jeon, J. Eng. Mech. **129**, 21 (2003).
[7] P. S. Plummer and V. A. Gostin, J. Sediment. Petrol., **51**, 1147 (1981).
[8] R. Weinberger, J. Struct. Geol. **21**, 379 (1999).
[9] V. Y. Chertkov, Eur. J. Soil. Sci., **53**, 105 (2002).
[10] T. Akiyama, H. Liu, and K-I. Hayakawa, Int. J. Heat Mass Transfer **40**, 1601 (1997).

[11] W. Kang and N-Ho. Lee, Wood Sci. Technol. **36**, 463 (2002).
[12] E. A. Jagla and A. G. Rojo, Phys. Rev. E **65**, 026203 (2002).
[13] R. Saliba and E. A. Jagla, J. Geophys. Res. **108**, 2476 (2003).
[14] M. Dance, P. L. Hancock, R. S. J. Sparks, and A. Wallman, J. Struct. Geol. **23**, 165 (2001).
[15] R. S. Sletten, B. Hallet, and R. C. Fletcher, J. Geophys. Res. **108**, 8044 (2001).
[16] R. Loison, P. Foch, and A. Boyer, *Coke: Quality and Production*, 2nd ed. (Butterworths, London, 1989).
[17] S. Nemat-Nasser, L. M. Keer, and K. S. Parihar, Int. J. Solids Struct., **14**, 409 (1978).
[18] S. Nemat-Nasser, Y. Sumi, and L. M. Keer, Int. J. Solids Struct. **16**, 1017 (1980).
[19] Z. P. Bažant, H. Ohtsubo, and K. Aoh, Int. J. Fract., **15**, 443 (1979).
[20] H-A. Bahr, H-J. Weiss, H. G. Maschje, and F. Meissner, Theor. Appl. Fract. Mech., **10**, 219 (1988).
[21] H-A. Bahr, U. Bahr, and A. Petzold, Europhys. Lett., **19**, 485 (1992).
[22] H. S. Carslaw and J. C. Jaeger, *Conduction of Heat in Solids*, 2nd ed. (Clarendon, Oxford, 1959).
[23] E. A. Jagla, Phys. Rev. E **65**, 046147 (2002).
[24] B. R. Lawn and T. R. Wilshaw, *Fracture of Brittle Solids* (Cambridge University Press, Cambridge, England, 1975).
[25] A. Groisman and E. Kaplan, Europhys. Lett., **25**, 415 (1994).
[26] K. A. Shorlin, J. R. de Bruyn, M. Graham, and S. W. Morris, Phys. Rev. E **61**, 6950 (2000).
[27] E. A. Brener, H. Müller-Krumbhaar, and R. Spatschek, Phys. Rev. Lett. **86**, 1291 (2001).
[28] G. Müller, J. Geophys. Res., **103**, 15293 (1998).
[29] G. Müller, J. Volcanol. Geotherm. Res., **86**, 93 (1998).
[30] A. Toramaru and T. Matsumoto, J. Geophys. Res. **109**, B02205 (2004).
[31] M. Mahoney, D. R. Jenkins, J. Keating, A. LeBas, and S. McGuire, *Factors Affecting Coke Size and Fissuring During Cokemaking*, Proceedings of the 2nd International Meeting on Ironmaking, Brazil, 2004 (Associacao Brasileira de Metalurgia e Materiais, 2004), pp. 871–880.